VIRTUAL STAINING FROM OPTICAL COHERENCE TOMOGRAPHY TO HEMATOXYLIN AND EOSIN STAINED SKIN TUMOR SAMPLES IN PETS

***Daira Viškere[1,3], Diāna Dupļevska[2], Ilze Matīse-van Houtana[1,3], Romans Maļiks[2], Roberts Kadiķis[2], Blaž Cugmas[1], Mindaugas Tamošiūnas[1]**
[1]University of Latvia, Latvia
[2]Institute of Electronics and Computer Science, Latvia
[3]Latvia University of Life Sciences and Technologies, Latvia
*Corresponding author's e-mail: daira.viskere@gmail.com

Abstract
Recently, virtual staining has revolutionized histopathology by utilizing AI for efficient H&E staining, reducing the need for specialized personnel. The use of virtual staining in veterinary medicine, particularly in transitioning from OCT to H&E, is inadequately addressed in current research. We employed generative adversarial networks to convert OCT images from canine and feline soft tissue sarcoma paraffin blocks into representations akin to H&E staining. The models were trained on 512x512 pixel paired and unpaired image patches, using a manually H&E stained image as a reference and OCT images as inputs. The neural network model employing transfer learning failed to attain microscopic accuracy, necessitating a complete retraining without transfer learning. Subsequent evaluations with Pix2Pix yielded no improvements, prompting a transition to ResNet, U-net, and Dense U-net architectures, which also did not enhance performance. This study aimed to ascertain the feasibility of utilizing the existing OCT database to generate pilot virtual staining on C-scan images through neural networks. Given that our output images did not yield satisfactory results for veterinary oncology, further research is imperative to optimize the neural network for virtually stained OCT images, with a focus on enhancing the OCT dataset.
Keywords: OCT, veterinary oncology, neural networks, non-invasive imaging, tumor diagnostics.

Introduction

Recently, virtual staining (VS) has transformed the histopathology field, where specially trained artificial intelligence (AI) employs standard H&E (hematoxylin and eosin) staining as a reference (Li et al., 2021; Tavolara et al., 2023). In veterinary oncology, histopathology plays important role because it has been accepted as gold standard. But because of several important facts (sampling needs anesthesia, it is invasive procedure and, for obtaining results, time is needed), OCT (Optical Coherence Tomography) has demonstrated potential as an efficient technique which is more advanced because that can produce real-time, non-invasive tissue evaluation, outlining tumor margins during surgery and even assisting in tumor type diagnosis (Ribeiro et al., 2022).

Thus far, OCT has been used for evaluating normal skin structures in humans and various animals, as well as skin lesions with dermatological and oncological diseases (Winetraub et al., 2024). In veterinary oncology, OCT has been utilized for skin and subcutaneous tumors, demonstrating the capability to distinguish these tumors to a certain percentage accuracy (Cugmas et al., 2021).

VS in veterinary oncology leverages advanced deep learning techniques to digitally replicate traditional histological staining processes, offering a more efficient, cost-effective, and environmentally friendly alternative. This approach accelerates diagnosis, which is crucial for both - patients and veterinarians, and is environmentally sustainable by minimizing the need for chemical stains. This method involves training neural networks to transform unstained or differently stained tissue images into VS images that mimic conventional stains like H&E (Dupļevska et al., 2024) or immunohistochemical stains (Lahiani et al., 2019).

VS often employs generative adversarial networks (GAN), such as the Pix2Pix model, designed for image-to-image translation when paired datasets are available. In the context of virtual staining in veterinary medicine, Pix2Pix can be trained to convert images from unlabeled tissue images into virtually stained images that resemble traditional histological stains or translate multispectral fluorescence images into brightfield represantations without physically applying dyes (Isola et al., 2017). This approach helps save time and resources, and reduces the need for tissue destruction, what is crucial in veterinary oncology for diagnosing and surgically approaching tumors (Rivenson et al., 2019, 2020).

Beyond Pix2Pix, GANs in general are advanced neural networks that create realistic synthetic data by competing two models—the generator and the discriminator.

CycleGAN extends this concept to perform unpaired image translation. It is a type of artificial intelligence model used to translate images from one style or domain to another without needing exactly matched images (paired examples) (Zhu et al., 2020), which is especially useful when paired data is scarce. This capability is useful for enhancing diagnostic visualization, standardizing images from different sources, or creating digital stains that mimic traditional laboratory techniques, all while preserving important tissue details.

ResNet or Residual Network is a deep neural network architecture that is designed for transformation between structurally similar but visually different images (Xu et al., 2023b) and when trained effectively is often used for image classification tasks, such as diagnosing diseases from medical images. It includes 'skip connections' that help the network learn better by

preventing issues like vanishing gradients. When integrated with ResNet – forming CycleGAN with ResNet – the model gains deeper learning capacity and better detail preservation, improving the quality of virtually stained images.

For segmentation purposes during virtual staining or image analysis, architectures like U-Net are widely used to precisely delineate tissue structures. U-Net is a type of neural network which has an encoder-decoder architecture: the encoder captures context by progressively downsampling the image, while the decoder restores the spatial details and combines them with features from earlier stages through skip connections. This design enables precise localization even with limited training data. It is designed for image segmentation, which means it helps to precisely locate and outline features within images. It's widely used in medical and histological imaging because it helps to identify and outline specific structures within images, such as tissues or cells and can accurately segment complex shapes even with limited training data.

An even more advanced version, Dense U-Net, incorporates dense connections to improve feature reuse and segmentation accuracy. These models enable better visualization by improving the accuracy and color balance of the VS images (Dupļevska et al., 2024) and therefore improving diagnosis by accurately isolating specific tissue components in the virtually stained images.

Advanced neural networks can be re-trained using transfere learning (TL) to replicate immunohistochemical stains on unstained samples, enabling differentiation of tumor types where traditional histopathology falls short (Cho et al., 2017). TL is a powerful approach in deep learning that enables a pre-trained model to be adapted to a new task (Xu et al., 2023a).

The application of TL for VS from optical coherence tomography to H&E stained samples in veterinary medicine has not been explicitly documented in the provided research papers. The papers primarily focus on human medical applications, utilizing deep learning techniques to transform histological images from one stain type to another (Bai et al., 2023; Latonen et al., 2024). These studies highlight the potential of virtual staining in enhancing diagnostic workflows and reducing the need for physical staining processes, but they do not specifically address veterinary applications.

While the field currently focuses on human applications, the methodologies and technologies developed could potentially be adapted for veterinary medicine. In contrast to the focus on human medical applications, the potential for virtual staining in veterinary medicine remains largely unexplored in the current literature. The adaptation of these techniques to veterinary medicine would require the collection and annotation of veterinary-specific histological data to train the models effectively. This adaptation could lead to significant advancements in veterinary pathology, similar to those seen in human medicine.

By combining OCT with virtual staining, several benefits can be achieved, including rapid acquisition of real-time histological images in a non-invasive manner (Winetraub et al., 2021). Images can be obtained from multiple sites and sections as needed and sent digitally to a pathologist immediately after capture, potentially receiving feedback during surgery - thereby optimizing surgical technique and scope based on the acquired results. This integration of OCT and virtual staining could significantly enhance the accuracy of surgical margin assessment and improve patient outcomes in veterinary oncology (Fabelo et al., 2021). While early diagnosis and treatment are critical, there is a concern regarding the risks associated with anesthesia for histopathological sampling, which may lead to suboptimal surgical decisions if not properly managed. In some cases, it could help to distinguish between surgical and non-surgical treatment as appropriate depending on tumor type and location (De Nardi et al., 2022). Further exploration of the integration of OCT and virtual staining could lead to groundbreaking advancements in veterinary surgical oncology, ultimately benefiting both animal patients and their owners.

The goal of this study was to understand if the current OCT database could be used to produce the pilot virtual staining (based on the neural networks) on our C-scan images. We observed that STS tumor cells appear brighter in OCT images and hypothesized that the tumor becomes distinctive by applying the virtual staining.

Materials and Methods

Preparation of tumor samples

Formalin-fixed tumor samples were obtained from the biopsy submissions to a commercial veterinary pathology laboratory (Matise Veterinary Pathology service, Riga, Latvia). These samples originated from client-owned dogs and cats for which the veterinarian-clinician recommended excisional surgery. The details of the tumor sample preparation, processing and histopathological examination procedure have been reported previously (Dupļevska et al., 2024) with exception that histological sections after cutting were deparaffinized, stained with hematoxylin and eosin and coverslipped.

After trimming, skin tissue samples that were diagnosed as cancer (soft tissue sarcoma) in feline and canine submissions, were stored in 10% formalin and provided to veterinary pathology laboratory for tissue blocks preparation and histological sections staining with hematoxylin and eosin. In addition, detailed assessment of tumor in corresponding H&E stained histological sections was performed by a board-certified veterinary pathologist Ilze Matīse-van Houtana (Matise Veterinary

Pathology service, Riga, Latvia). Tissue paraffin blocks from 51 soft tissue sarcomas samples were used for further analysis by OCT scanning at Biophotonics laboratory (University of Latvia).

Image registration

Spectral-domain OCT (sd-OCT) images were acquired using Telesto II (Thorlabs, Newton, NJ, USA) OCT device equipped with 1325 nm/100 nm spectral bandwidth SLD excitation light source, yielding ~ 8-micron axial resolution in tissue. The lateral resolution of OCT-LK2 telecentric scan-lens (EFL = 18 mm Thorlabs) was ~7 μm. The tissue sample from paraffin block was placed on the OCT sample holder and the 3D OCT image cube was acquired comprising the multiple B-scan images, keeping the beam focus point approximately 50 μm below the tissue surface and slightly tilting the samples. Galvanometric mirror-based scan stage operated at a 5 kHZ scan rate, and used the maximum number of 20 A-scans and 6 B-scans for the averaging. The pixel size in XY direction was set manually for 2 microns and the pixel size in z direction was 2.25 microns. The OCT images were collected in 1 x 1 mm scan area, and up to 2 mm penetration depth. ThorImage OCT software (Thorlabs) was used to perform volume rendering of z-stacked OCT data, displaying the grayscale view within 20-95 dB dynamic range, and subsequently extracting and storing the 2D cross sectional XY plane images across the sample in png format. *Ex vivo* STS tissue block samples, prepared using standard paraffin technique, were analysed by OCT. The image features within the top crossectional XY plane from each 3D OCT rendering were correlated with histological structures identified in H&E stained slides, appearing as the mirror images to the corresponding cross sections in OCT.

Image preprocessing

Prior to feeding the raw data to the proposed neural network, it needs to be processed and registered. Thus, both OCT image data and H&E stained brightfield image data were spatially aligned. The raw input STS images were extracted with the open-source OpenSlide library. During the research, the necessity of both (OCT and H&E brightfield) raw data type pre-processing was established. The H&E stained data underwent only background pixel color standardization (white color) as this type of images was chosen as those that are referenced to during the registration process.

Initially, processed images were converted to grayscale. Then, the proposed algorithm initialized the ORB detector that detected keypoints and extracted descriptors for each image. The code created a descriptor matcher and matched descriptors between the two images using the Hamming distance. In addition, we filtered and matched descriptors based on their distances, discarding the matches that exceeded the chosen threshold. Finally, the algorithm extracted the corresponding keypoints from the matched keypoints.

When the matching process was completed, the RANSAC (Random Sample Consensus) algorithm (Derpanis, 2010) was used to find the homography matrix, which represents the transformation between the two images. Then the computed homography was applied to warp the OCT image and align it with the H&E stained one, resulting in the registered image data. The final step before using the registered data for the further virtual staining process was to split each image pair into tiles of 512×512 pixels.

Virtual staining

Since the images used for training were not automaticly paired, but same regions were manually cropped, where their accuracy cannot be objectively measured, several approaches were tested. First approach where we assumed that the manually marked areas do not form pairs and do not exactly match each other. We tried transfer learning in virtual staining tasks. Transfer learning was employed to investigate the applicability of previously trained virtual staining model originally trained on fluorescence images stained with H&E to a different input - OCT images (Dupļevska et al., 2024). The use of transfer learning aimed to evaluate whether a pre-trained model could generalize well enough to produce histologically meaningful virtual stains on new data without further fine-tuning or parameter adjustment.

As we speculated that the images could be paired by manual selection, an attempt was made to train the neural network anew without transfer learning using previous methods.

Additionally, the standard Pix2Pix architecture without dense components was tested. This is a classic Pix2Pix model with no prior customization.

After that, a modified Pix2Pix framework, a type of conditional generative adversarial network (cGAN) was used where the generator was based on a Dense U-Net architecture. The Dense U-Net replaced standard convolutional blocks with densely connected layers to enhance feature propagation and preserve fine tissue structures, such as nuclei and connective tissue boundaries. The model was trained on paired datasets consisting of multispectral fluorescence images (captured in DAPI) and their corresponding manually H&E-stained brightfield images. Training was performed on image patches of 512×512 pixels over 40 epochs, using 800 patches for training and 200 for validation. To stabilize training and improve detail retention, further enhancements were applied to both the generator and discriminator, including the use of instance normalization and spectral normalization.

CycleGAN with U-Net approach the ResNet connections in the CycleGAN architecture were replaced with U-Net connections.

Results and Discussion

In our case, transfer learning strategy in virtual staining tasks was particularly relevant for veterinary oncology, where access to labeled training data is limited and manual histological staining is time-consuming and resource-intensive.

Figure 1

Soft tissue sarcoma from dog - virtually stained with Pix2Pix dense transfer learning OCT

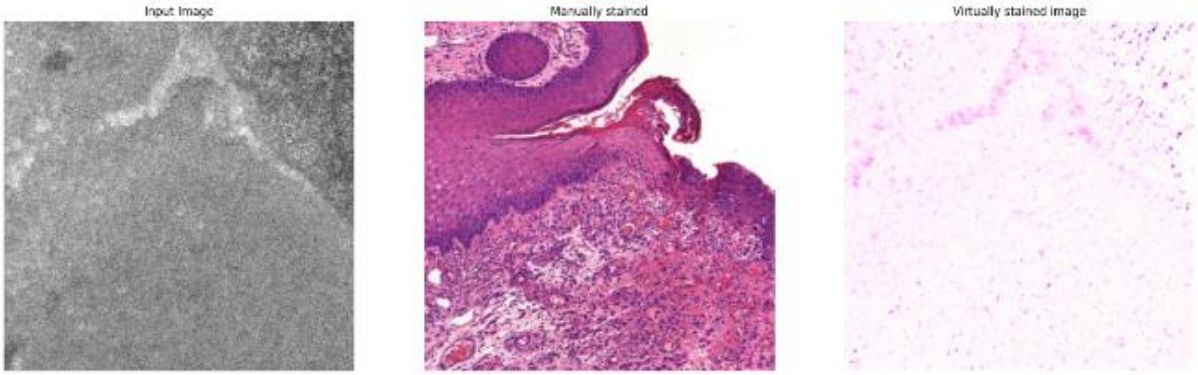

Results in Figure 1 showed that since OCT and brightfield images contain entirely different types of structural and spectral features, the neural network could interpret only the isolated pink dots representing the maxima. Training from scratch unfortunately did not produce positive results — the output of the model did not yield interpretable images, see 'Figure 2'.

Figure 2

STS virtually stained with Pix2Pix dense OCT

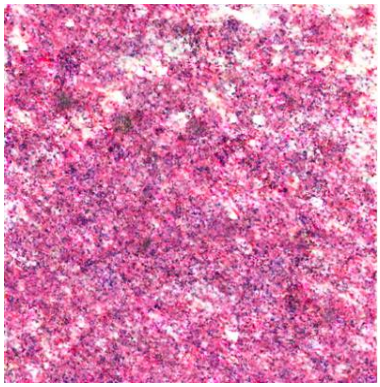

In our previous work with autofluorescence and H&E samples, classic Pix2Pix model with no prior customization performed poorly (Dupļevska et al., 2024). Similar results can be observed in Figure 3.

Since the input and reference images differ significantly in this case and are not exactly a paired set, the CycleGAN architecture was used. Using CycleGAN with ResNet the VS image began to display contours and cell edges, and resembled the structure of OCT sample, see 'Figure 4'.

Figure 3

STS virtually stained with Pix2Pix U-net OCT

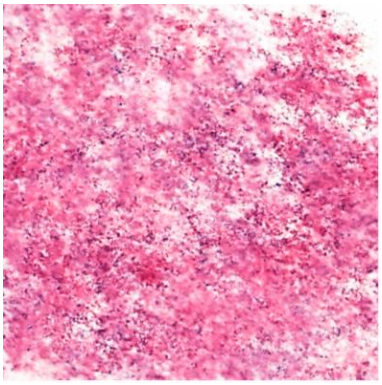

Figure 4

STS virtually stained with CycleGAN with ResNet

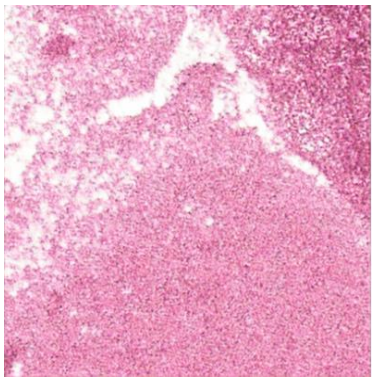

In CycleGAN with U-Net approach, the result was worse than in CycleGAN with ResNet because virtually stained image lost some structural details, Figure 5.

Figure 5
STS virtually stained with CycleGAN with U-net OCT

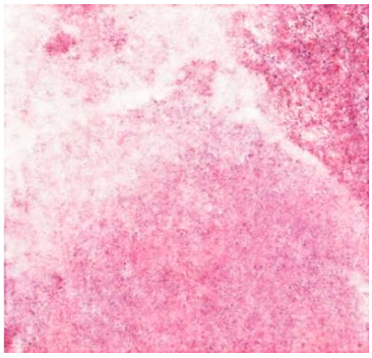

Dense U-Net architecture without ResNet or U-Net blocks did not improve after CycleGAN with U-net was applied. In Figure 6, the virtually stained image did not achieve higher quality compared to the previous models.

Figure 6
STS virtually stained with CycleGAN with Dense U-Net

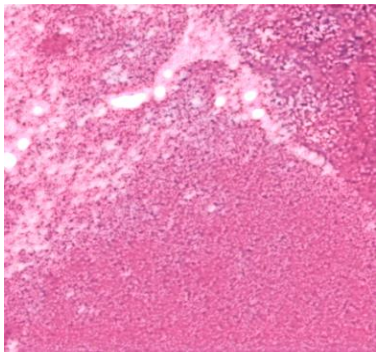

While VS promises numerous advantages, including reduced resource consumption and increased efficiency, other approaches should be applied instead or together with OCT. Preliminary work is especially challenging when there is no prior research done with veterinary samples. In future work, we plan to improve the results with the help of a larger dataset. Currently, we used 51 tumor sample slides, but other applications in the literature indicate that Pix2Pix and CycleGAN require 300+ slides. In future, we plan to pair the data automatically using algorithms, rather than manually to test additional neural networks models, to improve acquisition time, to test different optical modalities, as well as to apply transfer learning by utilizing OCT/H&E datasets from open repositories or pre-existing modalities and to apply trained models.

Conclusions

1. Virtual staining may standardize veterinary histopathology as a rapid, label-free alternative to traditional methods, necessitating improvements in pilot OCT to H&E virtual staining results for clinical acceptance.
2. Accelerating model development necessitates dataset-specific tuning and preprocessing.
3. Additional research is imperative for training neural networks on virtually stained OCT images, particularly focusing on the OCT dataset.

Acknowledgements

The research was funded by the Latvian Council of Science, project lzp-2022/1-0274 'Histological recognition and analysis of veterinary tumors surgical margins by using artificial intelligence and multimodal imaging' and supported by project 'Strengthening the Institutional Capacity of LBTU for Excellence in Studies and Research', funded by The Recovery and Resilience Facility.

References

Bai, B., Yang, X., Li, Y., Zhang, Y., Pillar, N., & Ozcan, A. (2023). Deep learning-enabled virtual histological staining of biological samples. *Light, Science & Applications*, *12*(1), 57. https://doi.org/10.1038/s41377-023-01104-7

Cho, H., Lim, S., Choi, G., & Min, H. (2017). *Neural Stain-Style Transfer Learning using GAN for Histopathological Images* (arXiv:1710.08543). arXiv. https://doi.org/10.48550/arXiv.1710.08543

Cugmas, B., Viškere, D., Čiževskis, O., Melderis, M., Rubins, U., & Tamosiunas, M. (2021). Optical coherence tomography and Raman spectroscopy for ex vivo characterization of canine and feline skin and subcutaneous tumors: Preliminary results. *Optical Biopsy XIX: Toward Real-Time Spectroscopic Imaging and Diagnosis*, Article 11636, 20–26.

De Nardi, A. B., Dos Santos Horta, R., Fonseca-Alves, C. E., De Paiva, F. N., Linhares, L. C. M., Firmo, B. F., …, & Dagli, M. L. Z. (2022). Diagnosis, Prognosis and Treatment of Canine Cutaneous and Subcutaneous Mast Cell Tumors. *Cells*, *11*(4), 618. https://doi.org/10.3390/cells11040618

Derpanis, K. G. (2010). *'Overview of the RANSAC Algorithm'.* Version 1.2, York University. http://www.cse.yorku.ca/~kosta/CompVis_Notes/ransac.pdf

Dupļevska, D., Maļiks, R., Tamošiūnas, M., Melderis, M., Viškere, D., Cugmas, B., …, & Matīse-van Houtana, I. (2024). Interpreting microscopic structures in virtually stained histological sections for veterinary oncology applications. *Advanced Biomedical and Clinical Diagnostic and Surgical Guidance Systems XXII*, Article 12831, 113–128. https://doi.org/10.1117/12.3023420.short

Fabelo, C., Selmic, L. E., Huang, P., Samuelson, J. P., Reagan, J. K., Kalamaras, A., …, & Boppart, S. A. (2021). Evaluating optical coherence tomography for surgical margin assessment of canine mammary tumours. *Veterinary and Comparative Oncology*, *19*(4), 697–706. https://doi.org/10.1111/vco.12632

Isola, P., Zhu, J.-Y., Zhou, T., & Efros, A. A. (2017). *Image-To-Image Translation With Conditional Adversarial Networks*. 1125–1134. https://openaccess.thecvf.com/content_cvpr_2017/html/Isola_Image-To-Image_Translation_With_CVPR_2017_paper.html

Lahiani, A., Gildenblat, J., Klaman, I., Albarqouni, S., Navab, N., & Klaiman, E. (2019). *Virtualization of Tissue Staining in Digital Pathology Using an Unsupervised Deep Learning Approach* (pp. 47–55). https://doi.org/10.1007/978-3-030-23937-4_6

Latonen, L., Koivukoski, S., Khan, U., & Ruusuvuori, P. (2024). Virtual staining for histology by deep learning. *Trends in Biotechnology*, *42*(9), 1177–1191. https://doi.org/10.1016/j.tibtech.2024.02.009

Li, J., Garfinkel, J., Zhang, X., Wu, D., Zhang, Y., de Haan, K., …, & Ozcan, A. (2021). Biopsy-free in vivo virtual histology of skin using deep learning. *Light: Science & Applications*, *10*(1), Article 1. https://doi.org/10.1038/s41377-021-00674-8

Ribeiro, P. R., Bianchi, M. V., Bandinelli, M. B., Rosa, R. B., Echenique, J. V. Z., Serpa Stolf, A., …, & Pavarini, S. P. (2022). Pathological aspects of cutaneous mast cell tumors with metastases in 49 dogs. *Veterinary Pathology*, *59*(6), 922–930. https://doi.org/10.1177/03009858221114468

Rivenson, Y., Wang, H., Wei, Z., de Haan, K., Zhang, Y., Wu, Y., …, & Ozcan, A. (2019). Virtual histological staining of unlabelled tissue-autofluorescence images via deep learning. *Nature Biomedical Engineering*, *3*(6), Article 6. https://doi.org/10.1038/s41551-019-0362-y

Rivenson, Y., De Haan, K., Wallace, W. D., & Ozcan, A. (2020). Emerging Advances to Transform Histopathology Using Virtual Staining. *BME Frontiers*, 2020, Article 9647163. https://doi.org/10.34133/2020/9647163

Tavolara, T. E., Su, Z., Gurcan, M. N., & Niazi, M. K. K. (2023). One label is all you need: Interpretable AI-enhanced histopathology for oncology. *Seminars in Cancer Biology*, 97, 70–85. https://doi.org/10.1016/j.semcancer.2023.09.006

Winetraub, Y., Yuan, E., Terem, I., Yu, C., Chan, W., Do, H., …, & Hong, M. (2021). OCT2Hist: Non-invasive virtual biopsy using optical coherence tomography. *MedRxiv*, 2021–03.

Winetraub, Y., Van Vleck, A., Yuan, E., Terem, I., Zhao, J., Yu, C., …, & de la Zerda, A. (2024). Noninvasive virtual biopsy using micro-registered optical coherence tomography (OCT) in human subjects. *Science Advances*, *10*(15), Article 5794. https://doi.org/10.1126/sciadv.adi5794

Xu, W., Fu, Y.-L., & Zhu, D. (2023a). ResNet and its application to medical image processing: Research progress and challenges. *Computer Methods and Programs in Biomedicine*, 240, Article 107660. https://doi.org/10.1016/j.cmpb.2023.107660

Xu, X., Xiao, Z., Zhang, F., Wang, C., Wei, B., Wang, Y., …, & Xu, F. (2023b). CellVisioner: A Generalizable Cell Virtual Staining Toolbox based on Few-Shot Transfer Learning for Mechanobiological Analysis. *Research*, 6, Article 0285. https://doi.org/10.34133/research.0285

Zhu, J.-Y., Park, T., Isola, P., & Efros, A. A. (2020). *Unpaired Image-to-Image Translation using Cycle-Consistent Adversarial Networks* (arXiv:1703.10593). arXiv. https://doi.org/10.48550/arXiv.1703.10593